Connolly, J.P.R., Turner, N.C.A., Hallam, J., Rimbi, P.T., Flett, T., McCormack, M.J., Roe, A.J. and O'Boyle, N. (2021) D-serine induces distinct transcriptomes in diverse Escherichia coli pathotypes. *Microbiology*, 167(10), 001093. (doi: 10.1099/mic.0.001093).

This is the author's final accepted version.

There may be differences between this version and the published version. You are advised to consult the publisher's version if you wish to cite from it.

http://eprints.gla.ac.uk/249636/

Deposited on: 16 August 2021

Enlighten – Research publications by members of the University of Glasgow
http://eprints.gla.ac.uk

D-serine induces distinct transcriptomes in diverse *Escherichia coli* pathotypes

James P. R. Connolly[1^], Natasha C. A. Turner[2^], Jennifer C. Hallam[2^], Patricia T. Rimbi[2], Tom Flett[2], Mhairi J. McCormack[2], Andrew J. Roe[2*] and Nicky O'Boyle[2*]

[1] Newcastle University Biosciences Institute, Newcastle-upon-Tyne, NE2 4HH, United Kingdom

[2] Institute of Infection, Immunity and Inflammation, University of Glasgow, Glasgow, G12 8TA, United Kingdom

[^]These authors contributed equally to this work

*Correspondence:

Nicky.oboyle@glasgow.ac.uk Tel: 01413307264

Andrew.roe@glasgow.ac.uk Tel: 01413302980

Key words – D-amino acids, Regulation, *E. coli*, Transcriptome

Word Count – 2735

Abstract

Appropriate interpretation of environmental signals facilitates niche specificity in pathogenic bacteria. However, the responses of niche-specific pathogens to common host signals are poorly understood. D-serine (D-ser) is a toxic metabolite present in highly variable concentrations at different colonisation sites within the human host that we previously found is capable of inducing changes in gene expression. In this study, we made the striking observation that the global transcriptional response of three *Escherichia coli* pathotypes - enterohaemorrhagic *E. coli* (EHEC), uropathogenic *E. coli* (UPEC) and neonatal meningitis associated *E. coli* (NMEC) - to D-ser was highly distinct. In fact, we identified no single differentially expressed gene common to all three strains. We observed the induction of ribosome-associated genes in extraintestinal pathogens UPEC and NMEC only, and the induction of purine metabolism genes in gut-restricted EHEC, and UPEC indicating distinct transcriptional responses to a common signal. UPEC and NMEC encode *dsdCXA* – a genetic locus required for detoxification and hence normal growth in the presence of D-ser. Specific transcriptional responses were induced in strains accumulating D-ser (WT EHEC and UPEC/NMEC mutants lacking the D-ser-responsive transcriptional activator DsdC), corroborating the notion that D-ser is an unfavourable metabolite if not metabolized. Importantly, many of the UPEC-associated transcriptome alterations correlate with published data on the urinary transcriptome, supporting the hypothesis that D-ser sensing forms a key part of urinary niche adaptation in this pathotype. Collectively, our results demonstrate distinct pleiotropic responses to a common metabolite in diverse *E. coli* pathotypes, with important implications for niche selectivity.

Materials and Methods

Bacterial growth conditions

All strains (listed in Table S1) were routinely cultured at 37°C in LB (Miller's recipe – 10 g L^{-1} NaCl). For growth assays and transcriptomic analysis, LB overnight cultures were diluted 1/100 in M9 minimal medium with 0.4% (w/v) glucose and incubated at 37°C, 200 rpm. At the indicated timepoints, D-ser was added to a final concentration of 1 mM. After an additional 2 h in the presence or absence of D-ser, 1 ml aliquots were taken and centrifuged at 10,000 × *g* before resuspending in RNA Later Reagent (Thermofisher). MOPS minimal medium (Teknova) with 15 g L^{-1} agar and 0.4% D-ser as a sole carbon source was used to test for catabolism of D-ser.

Construction of isogenic dsdC deletion mutants and complemented strains

A list of plasmids and primers used in this study is included in Tables S2 and S3 respectively. Deletion mutants were constructed using Lambda Red mutagenesis [1], briefly summarised as follows. Each strain was transformed with pKD46 and cultured in super optimal broth (SOB) with 100 µg ml^{-1} ampicillin to $OD_{600\ nm}$ 0.1. L-arabinose was added to a final concentration of 10 mM and incubation was continued for 45 min. Cells were harvested by centrifugation, washed three times with ice-cold distilled water and electroporated with 1 µg of each Lambda Red PCR fragment (Constructed using red.F and red.R primers with pKD4 serving as a PCR template [Tables S2 and S3]). Following selection on LB with 40 µg ml^{-1} kanamycin, mutants were verified by PCR using *dsdC*, *dsdC1* and *dsdC2*-check-F and check-R primers (Table S3), with molecular weight decreases of 523, 529 and 532 bp, respectively confirming each insertion. Resistance markers were eliminated by FLP recombination using pCP20

and verified by replica plating on LB and LB with 40 µg ml^{-1} kanamycin. For mutation of *dsdC1* and *dsdC2* in NMEC, the process was carried out first for *dsdC1* before repeating for *dsdC2*. For complementation, wild type alleles (including their native promoters) were amplified with primers *dsdC1*.184.F (CFT073 *dsdC* and CE10 *dsdC1*), *dsdC2*.184.F (CE10 *dsdC2*) and *dsdC*.184.R (all 3 alleles) and assembled into linearised pACYC184 (constructed by amplification with primers pACYC.lin.F and pACYC.lin.R) by virtue of compatible 5' ends using the NEB HiFi DNA Assembly kit (New England Biolabs). Resulting constructs p*dsdC*, p*dsdC1* and p*dsdC2* were sequence verified before transforming into the appropriate deletion mutant strains.

mRNA extraction and purification

Transcriptomic analysis was performed on three biological replicates of each strain in the presence and absence of 1 mM D-ser. RNA was extracted from stabilized cells using PureLink Mini RNA extraction kit according to manufacturer's instructions. RNA was eluted in 100 µl nuclease-free water. Genomic DNA was removed by incubating with 4 µl Turbo DNase (Thermofisher) for 1 h at 37°C. Nucleic acid was extracted with phenol-chloroform-isoamyl alcohol and ethanol precipitated with 2 µl Glycoblue (Thermofisher) overnight at -80°C. RNA was collected by centrifugation at 17,000 × *g*, 4°C for 30 min before washing with 70% ethanol and resuspending in TE buffer. RNA was checked for DNA contamination by PCR using *groEL*-F and *groEL*-R primers (Table S3). RNA integrity was confirmed by Agilent Bioanalyzer 2100. Ribosomal RNA was removed using MICROBExpress mRNA enrichment kit (Thermofisher) according to manufacturer's instructions.

RNA sequencing

Library preparation and sequencing was performed at University of Glasgow Polyomics. Libraries were prepared using TrueSeq Stranded mRNA Library kit (Illumina) according to manufacturer's instructions. Illumina NextSeq 500 was employed for sequencing with 10 million 75 bp single end reads being obtained. Read quality was assessed with FastQC (Babraham Bioinformatics) - minimum Phred threshold of 20. Data were analysed using CLC Genomics Workbench (Qiagen). Reads were mapped to the EDL933, CFT073 and CE10 reference genomes (NCBI accession numbers: NC_002655.2; NZ_CP051263.1 and NC_017646.1 respectively) using default mapping parameters. Differential expression was assessed using the empirical analysis of differential expression (EdgeR). Genes having an absolute fold change of ≥ 1.5; ≤ -1.5 and a false-discovery rate (FDR) corrected *p*-value of ≤ 0.05 were considered significant (Dataset S1). Volcano plots were exported from CLC Genomics before coloring and adding labels in Photoshop Elements (Adobe). Datapoints having a FDR-corrected *p*-value of zero were manually added beyond the y-axis limit. Raw data has been uploaded to the ENA under accession numbers ERS4281309-ERS4281334 and ERS4281353-ERS4281356.

Data handling/functional category assignment

To identify genes commonly differentially expressed between pathotypes, the list of DEGs arising from D-ser exposure in each were first consulted. Where a match occurred and the direction of gene expression was the same, the DEGs were considered shared. Orthologous genes in different strains often carry distinct Genbank gene names/locus tags (e.g. *yhaU* and *garP* in EDL933 and CE10, respectively). As

such, where no direct gene name match was found, a nucleotide BLAST was performed, with a cut-off of 70% nucleotide identity across 70% of the sequence being considered an orthologous match. These data were used to construct the shared DEG matrices in Dataset S1. Again, the direction of gene expression was considered before constructing shared DEG Venn diagrams. Therefore, the genes considered uniquely differentially expressed in one pathotype over another comprise those not present in the other, those present but not differentially expressed, and those present but differentially expressed in the opposite direction. Functional categories were manually assigned to differentially expressed genes based on annotations derived from Colibase [2] and Uniprot [3] databases.

Results and Discussion

Pathogenic *Escherichia coli* comprise a diverse, ecologically specialized group of microorganisms capable of causing disease within the intestine – their primary site of colonization – but also at extraintestinal sites such as the brain and bladder. Our previous work described the incompatibility of enterohaemorrhagic *E. coli* (EHEC) with environments rich in the host metabolite D-ser [4]. Typically, EHEC cannot metabolize D-ser due to an evolutionary loss of *dsdC*, encoding the D-ser responsive transcriptional activator [5]. In addition to growth inhibition by D-ser, the expression of EHECs primary colonisation apparatus, the locus of enterocyte effacement (LEE)-encoded type three secretion system is repressed. It has been reported that D-ser is concentrated in the hippocampus and frontal cortex of the brain where concentrations reach (0.35–0.25 μmol g^{-1}) [6–8], while concentrations of D-ser in human urine can

145 reach in excess of 1 mM [9]. By contrast, we have observed that the concentration of
146 D-ser in the mouse gut is approximately 1,000-fold lower than that described for
147 human urine at 1 µM [4], however enteric concentrations in humans are likely to vary
148 considerably with diet and further studies in this area are warranted. The toxicity of
149 D-ser to EHEC at high concentrations is hypothesised to be a key factor in restricting
150 EHEC to its preferred gut niche, where D-ser concentrations are extremely low.
151 Indeed, carriage of an intact *dsdCXA* locus for D-ser metabolism in EHEC is extremely
152 rare [4].
153
154 The role of D-ser in modulating transcription in EHEC has been extensively
155 investigated, however there are often important intraspecies distinctions in responses
156 to the same metabolite with implications within the context of infection [10–12]. Here
157 we describe the transcriptional response of uropathogenic and neonatal meningitis-
158 associated *E. coli* (UPEC and NMEC) to D-ser. Unlike EHEC, these pathotypes
159 typically encode *dsdCXA*, with NMEC strains often carrying two copies of the locus
160 [5]. This is believed to be important in pathogenesis in the bladder and brain where D-
161 ser concentrations are higher than that of the gut. We previously described how
162 exposure of EHEC to D-ser results in a global transcriptional shift affecting virulence
163 and inducing stress [4, 13]. We therefore hypothesised that D-ser could promote
164 distinct transcriptomes in pathotypes not susceptible to D-ser toxicity. The inclusion of
165 D-ser from 0 h in M9 minimal medium caused dramatic growth arrest in EHEC but not
166 in UPEC and NMEC (Fig. 1 A-C). In order to assess the transcriptional response of
167 actively growing populations of all three pathotypes to D-ser, we spiked 1 mM D-ser
168 into the media after 3 hours growth and sampled cells after 2 hours of exposure using

RNA-seq analysis. This greatly reduced the severity of growth inhibition in EHEC (Fig. 1A). Intriguingly, this also led to a transient drop in the UPEC growth rate but not NMEC (Fig. 1B and C), possibly as a result of differential metabolic adaptation to the use of D-ser as a carbon source. This surprising common growth inhibition phenotype observed in EHEC and UPEC was reflected by similar numbers of differentially expressed genes (DEGs) (162 and 140 respectively; Fig. 1D-G; Dataset S1). Contrastingly, NMEC growth was not significantly affected and only 55 D-ser-induced DEGs were identified. DEGs belonged predominantly to transport and metabolism/biosynthesis functional categories (Fig. S1). Surprisingly, UPEC and NMEC shared fewer common DEGs (12) than UPEC and EHEC, despite their shared ability to metabolize D-ser (14; Fig. 1G). Importantly, there were no DEGs in common between all three strains, highlighting the individuality in pathotype responses to this metabolite.

The most significantly affected functional categories in all three pathotypes were metabolism/biosynthesis, followed by transport (Fig. S1 and Dataset S1), however the composition of these categories varied significantly between strains. This was highlighted by the fact that the genes/gene clusters bearing the highest level of D-ser-dependent induction were unique to each strain. In EHEC, transport/metabolism of galactarate/glucarate (*gar*) was highly upregulated (Fig. 1D), whereas in UPEC the fimbrial gene *fmlA* – the major subunit of the virulence-associated F9 pilus [14] – was most induced (Fig. 1E) and in NMEC threonine biosynthesis (*thr*) was strongly activated (Fig. 1F). The most downregulated genes in EHEC were associated with curli synthesis (*csg*) and tryptophan biosynthesis (*trp*) (Fig. 1D), while in UPEC and

193 NMEC, a zinc chelator encoded by *zinT*, and zinc transporter *znuABC* were strongly
194 reduced in expression (Fig. 1 E and F). Several genes involved in purine metabolism
195 were upregulated in both EHEC and UPEC, while all three strains exhibited repression
196 of distinct acid tolerance genes. These included *cfa*, *kgtP*, and *phoH* in EHEC, *gadX*
197 in NMEC, *hdeABD*, *gadAB*, *ybaST* in UPEC, *yagU* in both EHEC and NMEC, and
198 *gadC* in both EHEC and UPEC. We predicted that many conserved genes would be
199 inversely regulated in EHEC compared with UPEC/NMEC based on D-ser
200 deamination capability, however only one DEG followed such a pattern – a CstA family
201 pyruvate transporter encoded by *yjiY/btsT* that was upregulated in EHEC and
202 repressed in UPEC and NMEC (Fig. 1E).
203
204 In addition to *fmlA*, several DEGs with characterized roles in pathogenesis were
205 affected by D-ser. In UPEC, genes belonging to both operons encoding the *pap* pilus
206 – P-type chaperone-usher fimbriae that are overrepresented in pyelonephritis isolates
207 and function by binding the globoside glycolipid receptor in the kidney [15] - were
208 repressed. We also observed a striking upshift in ribosomal protein/RNA gene
209 expression in UPEC and NMEC but not in EHEC. Several 50S (*rpl*) and 30S (*rps*)
210 ribosomal protein genes were upregulated in both pathotypes in response to D-ser
211 (Fig. 1E and F). Importantly, many UPEC responses to D-ser (including upregulation
212 of ribosomal genes, repression of *pap* pilus and activation of cold shock genes) have
213 also been reported in response to growth in human urine [16] or during mouse/human
214 urinary tract infection [16–18]. Upregulation of ribosomal genes is believed to play a
215 role in disease by facilitating rapid growth via increased translation [18]. Thus, these

findings support our hypothesis that D-ser sensing is crucial for recognition of the urinary niche by UPEC.

In order to explore the importance of D-ser catabolism, we performed a parallel transcriptome analysis using UPEC and NMEC strains deleted for *dsdC* (the D-ser responsive transcriptional activator gene required for D-ser metabolism[19]). Note, as mentioned above NMEC encodes two copies of *dsdC*, which were both deleted. As predicted, UPEC Δ*dsdC* and NMEC Δ*dsdC1*/*C2* displayed severe growth arrest in the presence of D-ser (Fig. 2A-C). Exposure resulted in 1345 DEGs in UPEC Δ*dsdC*, 24% of its gene content. Contrastingly, NMEC Δ*dsdC1/C2* displayed 357 DEGs in response to D-ser. The large-scale shift in gene expression in these mutants compared with WT EHEC (162 DEGs) reflects their observed incompatibility with D-ser accumulation (Fig. 2A and B). This is consistent with the observation that carriage of intact *dsdCXA* is extremely common in these extra-intestinal isolates [5, 20] and that they can inhabit environments abundant in D-ser, where detoxification is a prerequisite for success. Accordingly, UPEC Δ*dsdC* and NMEC Δ*dsdC1*/*C2* displayed induction of greater numbers of stress response genes than their wild type counterparts upon D-ser exposure and accumulation. While some overlap was observed in the responses of WT and *dsdC* mutants to D-ser (including ribosome associated genes – suggesting a sensing mechanism independent of accumulation), the response of the mutants was largely distinct (Fig. 2E). Comparison of *dsdC*-negative UPEC and NMEC mutant response with EHEC identified a core set of 30 D-ser accumulation-dependent DEGs (Fig. 2F). These include induction of galactarate transport and metabolism genes (*gar*), glycine cleavage system genes (*gcv*) (Fig. 2C

and D; Dataset S1). This subset of DEGs likely contributes specifically to the growth arrest phenotype associated with D-ser accumulation and is currently under investigation. Complementation of *dsdC* alleles in UPEC and NMEC deletion mutant backgrounds restored their ability to grow on MOPS minimal medium with D-ser as a sole carbon source (Fig. 2G), thereby confirming the targeted deletions as the specific cause of the growth phenotypes described in this study. It should be noted that the transcriptional response to stimulus is likely to vary over time, particularly in the case of metabolites that are subject to catabolism. Indeed, upregulation of *dsdXA*, the genes responsible for catabolism of D-ser was not observed in UPEC and NMEC 2 h after induction. This indicates that the transcriptional alterations observed here likely constitute the phase at which a proportion of the transcriptome of UPEC and NMEC has returned to baseline. While certain aspects of this transient/acute response to D-ser may be missing from these data, the indirect alterations in metabolism and physiology clearly influence transcription in a pathotype-specific manner up to 2 h post-treatment. Similarly, the small number of common DEGs between pathotypes corroborates the notion that a specific D-ser response remains at play

Conclusion

Exposure to D-ser resulted in distinct transcriptional responses in EHEC, UPEC and NMEC, highlighting the diverse strategies employed by different pathotypes in responding to a relevant environmental signal. Large scale subversion of global transcription occurred upon accumulation of D-ser, highlighting the strict requirement for detoxification in strains that occupy niches rich in this metabolite. Importantly, the data correlate with observations made from human studies of the UPEC transcriptome

during UTI, suggesting specific responses to D-ser as being highly relevant in a true physiological setting. These surprising nuances in transcriptional responses displayed by distinct but closely related pathotypes highlight the challenges faced when using single prototypic strains in drawing species-level conclusions.

Acknowledgements

We thank Julie Galbraith, David McGuinness and Graham Hamilton from University of Glasgow Polyomics for providing RNA sequencing and data upload services.

Funding Information

NO'B is supported by a Tenovus Scotland award. JPRC is supported by a Springboard award from the Academy of Medical Sciences [SBF005\1029]. AJR is supported by the Biotechnology and Biological Sciences Research Council [BB/M029646/1, BB/R006539/1].

Conflict of Interest Statement

The authors declare no conflict of interest.

References

1. **Datsenko KA, Wanner BL**. One-step inactivation of chromosomal genes in *Escherichia coli* K-12 using PCR products. *Proc Natl Acad Sci* 2000;97:6640 LP – 6645.
2. **Chaudhuri RR, Khan AM, Pallen MJ**. *coli* BASE: an online database for *Escherichia coli* , *Shigella* and *Salmonella* comparative genomics. *Nucleic*

Acids Res 2004;32:D296–D299.

3. **The UniProt Consortium**. UniProt: a hub for protein information. *Nucleic Acids Res* 2015;43:D204–D212.

4. **Connolly JPR, Goldstone RJ, Burgess K, Cogdell RJ, Beatson SA, *et al.*** The host metabolite D-serine contributes to bacterial niche specificity through gene selection. *ISME J* 2015;9:1039–1051.

5. **Moritz RL, Welch RA**. The *Escherichia coli argW-dsdCXA* genetic island is highly variable, and *E. coli* K1 strains commonly possess two copies of *dsdCXA. J Clin Microbiol* 2006;44:4038 LP – 4048.

6. **Hashimoto A, Oka T, Nishikawa T**. Anatomical distribution and postnatal changes in endogenous free D-aspartate and D-serine in rat brain and periphery. *Eur J Neurosci* 1995;7:1657–1663.

7. **Labrie V, Fukumura R, Rastogi A, Fick LJ, Wang W, *et al.*** Serine racemase is associated with schizophrenia susceptibility in humans and in a mouse model. *Hum Mol Genet* 2009;18:3227–3243.

8. **Nishikawa T**. Analysis of free D-serine in mammals and its biological relevance. *J Chromatogr B* 2011;879:3169–3183.

9. **Anfora AT, Haugen BJ, Roesch P, Redford P, Welch RA**. Roles of serine accumulation and catabolism in the colonization of the murine urinary tract by *Escherichia coli* CFT073. *Infect Immun* 2007;75:5298–5304.

10. **Johnson R, Ravenhall M, Pickard D, Dougan G, Byrne A, *et al.*** Comparison of *Salmonella enterica* serovars Typhi and Typhimurium reveals typhoidal serovar-specific responses to bile. *Infect Immun* 2018;86:e00490-17.

11. **Dogan B, Suzuki H, Herlekar D, Sartor RB, Campbell BJ, *et al.***

Inflammation-associated adherent-invasive *Escherichia coli* are enriched in pathways for use of propanediol and iron and M-cell translocation. *Inflamm Bowel Dis* 2014;20:1919–1932.

12. **Collins J, Robinson C, Danhof H, Knetsch CW, van Leeuwen HC, *et al.*** Dietary trehalose enhances virulence of epidemic *Clostridium difficile*. *Nature* 2018;553:291–294.

13. **Connolly JPR, Roe AJ**. Intracellular D-serine accumulation promotes genetic diversity via modulated induction of RecA in enterohemorrhagic *Escherichia coli*. *J Bacteriol* 2016;198:3318 LP – 3328.

14. **Conover MS, Ruer S, Taganna J, Kalas V, De Greve H, *et al.*** Inflammation-induced adhesin-receptor interaction provides a fitness advantage to uropathogenic *E. coli* during chronic infection. *Cell Host Microbe* 2016;20:482–492.

15. **Lane MC, Mobley HLT**. Role of P-fimbrial-mediated adherence in pyelonephritis and persistence of uropathogenic *Escherichia coli* (UPEC) in the mammalian kidney. *Kidney Int* 2007;72:19–25.

16. **Snyder JA, Haugen BJ, Buckles EL, Lockatell CV, Johnson DE, *et al.*** Transcriptome of uropathogenic *Escherichia coli* during urinary tract infection. *Infect Immun* 2004;72:6373 LP – 6381.

17. **Frick-Cheng AE, Sintsova A, Smith SN, Krauthammer M, Eaton KA, *et al.*** The gene expression profile of uropathogenic *Escherichia coli* in women with uncomplicated urinary tract infections is recapitulated in the mouse model. *MBio* 2020;11:e01412-20.

18. **Sintsova A, Frick-Cheng AE, Smith S, Pirani A, Subashchandrabose S, *et***

al. Genetically diverse uropathogenic *Escherichia coli* adopt a common transcriptional program in patients with UTIs. *Elife* 2019;8:e49748.

19. **Nørregaard-Madsen M, McFall E, Valentin-Hansen P**. Organization and transcriptional regulation of the *Escherichia coli* K-12 D-serine tolerance locus. *J Bacteriol* 1995;177:6456 LP – 6461.

20. **Roesch PL, Redford P, Batchelet S, Moritz RL, Pellett S, *et al.*** Uropathogenic *Escherichia coli* use D-serine deaminase to modulate infection of the murine urinary tract. *Mol Microbiol* 2003;49:55–67.

Figures

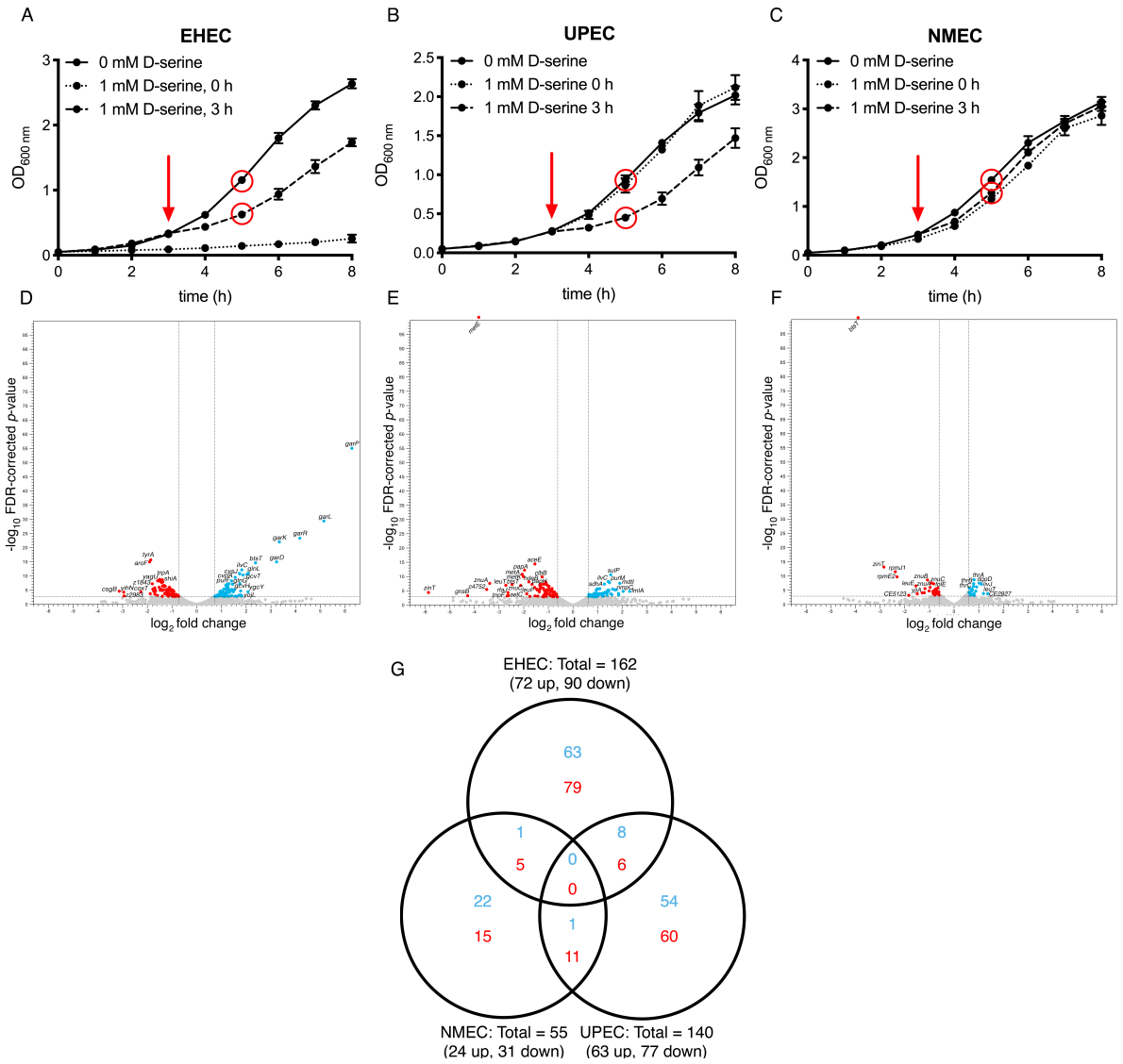

Fig. 1 Distinct growth and transcriptional responses of *E. coli* pathotypes to D-serine. (A-C) Growth curves of EHEC, UPEC and NMEC in the presence and absence of 1 mM D-ser, added at 0 h or 3 h (red arrow) post-inoculation as indicated. Dots indicate mean values from a minimum of three replicate experiments, with error bars indicating the SEM. Red circles indicate the timepoints and samples used for RNA-seq analysis. (D-F) Volcano plots depicting differential gene expression in EHEC, UPEC and NMEC, respectively, following 2 h exposure to 1 mM D-ser. Dots were manually added beyond the axis limits where FDR-corrected *p*-value of zero was obtained. Dotted lines indicate cut-off values for statistical significance (y-axis, $p < 0.05$) and fold-change (x-axis, fold > 1.5, < -1.5). Genes meeting these stringency criteria and induced by D-ser are coloured blue, while those repressed by D-ser are coloured red. (G) Venn diagram illustrating the distinction between genes differentially expressed following exposure to D-ser in three *E. coli* pathotypes. Numbers of genes increased in expression are coloured blue, while those decreased in expression are coloured red.

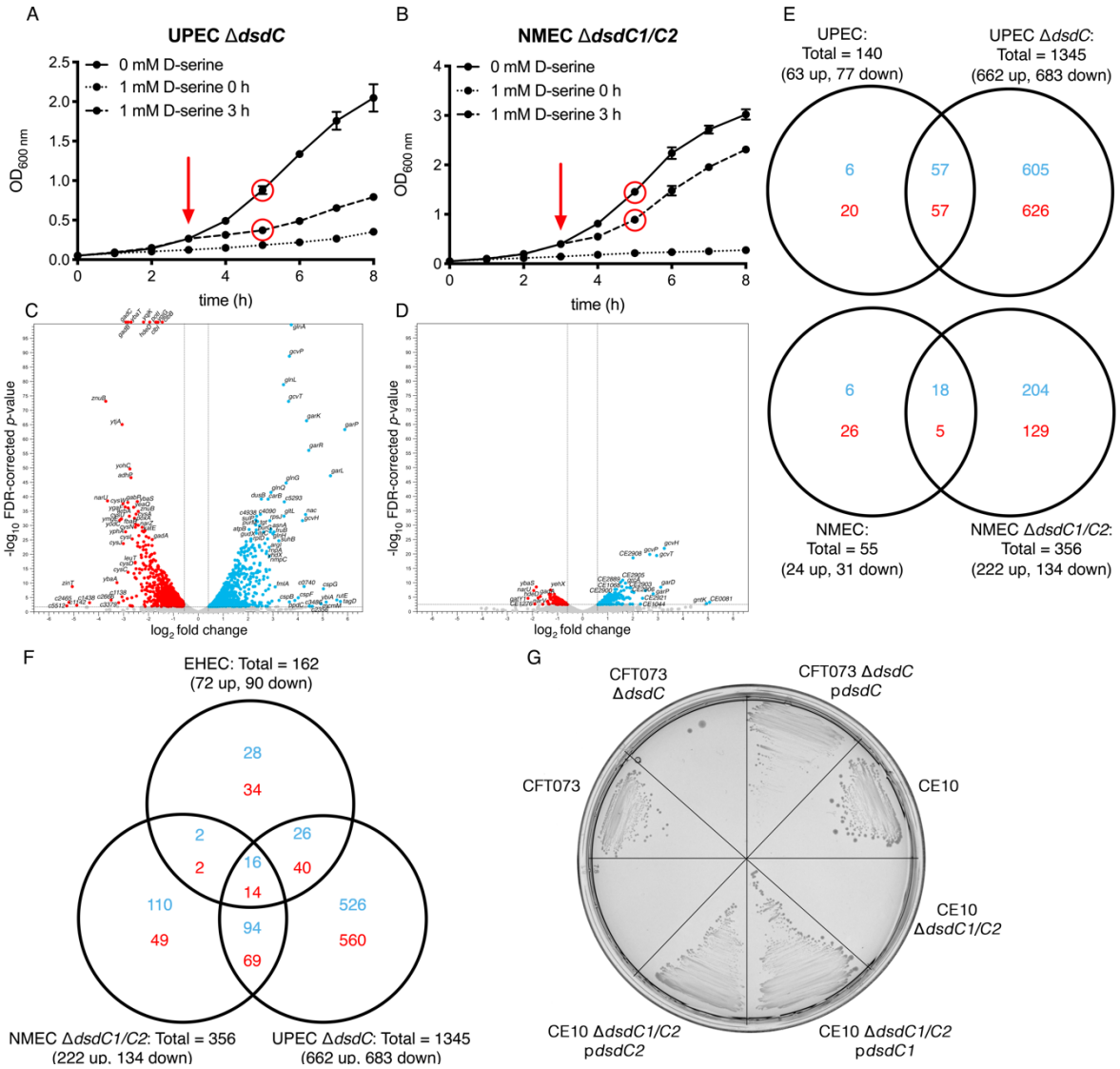

Fig. 2 Accumulation of D-ser has variable effects on UPEC and NMEC. (A and B) Growth curves of UPEC Δ*dsdC* and NMEC Δ*dsdC1/C2* in the presence and absence of 1 mM D-ser, added at 0 h or 3 h (red arrow) post-inoculation as indicated. Red circles indicate the timepoints and samples used for RNA-seq analysis. Dots indicate mean values from a minimum of three replicate experiments, with error bars indicating the SEM. (C and D) Volcano plots depicting differential gene expression following 2 h exposure to 1 mM D-ser. Dots were manually added beyond the axis limits where FDR-corrected *p*-value of zero was obtained. Dotted lines indicate cut-off values for statistical significance (y-axis, $p < 0.05$) and fold-change (x-axis, fold > 1.5, < -1.5). Genes meeting these stringency criteria and induced by D-ser are coloured blue, while those repressed by D-ser are coloured red. (E) Venn diagram illustrating comparing the effects of D-ser exposure in parental and DsdC-negative deletion mutants of UPEC and NMEC. (F) Venn diagram comparing genes differentially expressed after D-ser exposure in strains lacking DsdC. Numbers of genes increased in expression are coloured blue, while those decreased in expression are coloured red (E and F). (G) Growth of wild type, *dsdC* deletion mutant and trans complemented deletion mutants on MOPS 0.4% (w/v) D-ser (sole carbon source) plates after streaking an isolated colony and incubating at 37°C for 48 h.